Properties of the Transfers from LEO to the Retrograde-GEO using Lunar Swing-by in a Three-Body Model

Boyong He (heboyong@yeah.net)
State Key Laboratory of Astronautic Dynamics
Pengbin Ma
State Key Laboratory of Astronautic Dynamics
Hengnian Li
State Key Laboratory of Astronautic Dynamics

Research Article

Keywords: etrograde GEO, transfers, orbital property, lunar swing-by, orbit design, debris-warning

Posted Date: April 27th, 2021

DOI: https://doi.org/10.21203/rs.3.rs-464236/v1

Properties of the transfers from LEO to the retrograde-GEO using lunar swing-by in a three-body model

Boyong He[*,1], Pengbin Ma[1], Hengnian Li[1]

Abstract: A monitor-satellite on a retrograde geostationary earth orbit (retro-GEO) gives the GEO-assets debris-warnings per 12 hour. The properties of the transfers from a low earth orbit to the retro-GEO using lunar swing-by without middle-way maneuver are exhibited in a three-body model. Based on the Poincaré-section methodology, the proof of the existence of this transfer is proven in the planar circular restricted three-body problem (CR3BP) model. Then, the maximum altitude of the perilune of this transfer is solved using the sequence quadratic programming optimization algorithm. Besides, the orbital inclination changeable capacity of this transfer is calculated in the spatial CR3BP model by the continuation of the orbital design values in the planar CR3BP model. The numerical results show that the maximum altitude of the perilune is 892 km and the maximum orbital inclination changeable capacity is 138 degree relative to the plane of the Moon's path. Further analysis show that the minimum sum of the two-impulse velocity increments (i.e., departure from LEO and insert into the retro-GEO) is 4.224 km/s, the change of the orbital inclination is 107 degree relative to the plane of the Moon's path in this case. Due to the maximum angle of the plane of the Moon's path on the equator is 28.6 degree per Metonic cycle (i.e., 18.6 years), everyday has a month window to match the longitude of the launch-site for trans-lunar injection.

Keywords: retrograde GEO; transfers; orbital property; lunar swing-by; orbit design; debris-warning;

1 Introduction

As we known, the orbital period of the GEO is the same as the Earth's rotation period. Its sub-point coverage is almost still. Many important satellites for navigation, remote sensing, data-relay, meteorology, ocean monitoring and land and resources monitoring are deployed on the GEO. For decades, due to the exponential growth of the number of the GEO satellites, the rocket terminal stage, the failed-satellites, and the space debris, and the safety-domain limitation to accommodate perturbation, many important GEO positions deploys satellites under the co-location control. The GEO orbit is quite crowded, and the circumstance of these GEO-assets is serious. On July 28, 2014 and

[*] BY. He Corresponding author E-mail: heboyong@yeah.net
1. State Key Laboratory of Astronautic Dynamics (ADL), Xi'an Satellite Control Center, Xi'an, 710043, China.

August 19, 2016, the USA successfully launched four GEO satellites, GSSAP-1/2 and GSSAP-3/4 (Geosynchronous space Situational Awareness-Ness Program), respectively (Espinosa 2017). They were possible to give the GEO-assets neighborhood early debris-warning by raising or lowering the orbital altitude of themselves, but the fuel-cost of the orbital maneuvers greatly limited their patrol range. The retrograde geostationary earth orbit (retro-GEO) is a satellite orbit of the Earth, which has the same or a close orbital altitude as that of a GEO, but has an inclination of about 180 degree. A monitor-satellite on the retro-GEO gives all of the GEO-assets debris-warning per 12 hour. The transfer goes to a retro-GEO from a low earth orbit (LEO) using lunar swing-by as shown in Fig. 1. This flight manner avoids the difficulty of the westward-launch directly without ground-measurement and tracks facilities, in respect that the space missions are usual eastward-launch scenarios, and saves the launching energy-cost of counteracting the Earth's rotation.

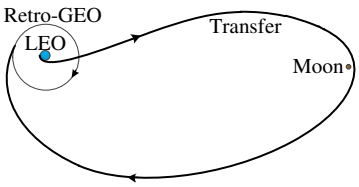

Fig. 1 Illustration of the transfer from LEO to the retrograde-GEO using lunar swing-by

The orbital dynamics description of the lunar swing-by dates back to *Issac Newton* in 1687. The circumlunar free-return orbit in Apollo mission is a famous practical activity to improve the safety of the crews in the manned space missions (Berry 1970). The probe *Hiten* launched by Japan in 1990 acted a double lunar swing-by space-flight (Uesugi 1990). In 1998, Hughes saved the original ISEE-3/ICE using multi-lunar swing-by and multi-maneuvers. It becomes the first successful space legend of saving satellites (Farquhar 2001). Zeng et al. (2000) studied the lunar swing-by transfer which launches up from a high-latitude launch-pad, flies to a GEO and a retro-GEO using the double two-body hypothesis. The results show that the transfer using lunar swing-by saves fuel-cost of maneuvers, but the perigee-altitude of the return-earth phase didn't match that of the retro-GEO. Luo et al. (2010) described the mechanics of the double lunar swing-by, expatiated the sensitive property of the transfers using the lunar swing-by to a certain extent.

As the number of the GEO satellites grows exponentially, the safety of GEO-assets caused by the abandoned-satellites and debris is becoming more and more serious (Oltrogge 2018). In 1984, Oberg (1984) presented the pioneering retro-GEO concept, and explained the flight-manner saves fuel-cost by

the lunar swing-by to deploy a satellite on the retro-GEO. Kawase et al. (2001; 2010) advanced the reasonable proposal that a monitor-satellite on the retro-GEO plays the debris-warning alertor for all of the GEO-assets. Aravind et al. (2012) compared the final left-fuel of the same satellite using typical flight-manners to the same retro-GEO with different number of maneuvers. They also tried to calculate the final left-fuel of the lunar swing-by flight-manner, but the perigee-altitude of the return-earth phase is 124.75 km, it is far below the desired orbital altitude of the retro-GEO.

To sum up, the retro-GEO gives all of the GEO-assets debris-warning per 12 hour, and the flight-manner saves fuel-cost to deploy a monitor-satellite to the retro-GEO by lunar swing-by. But, the cases until now in both reference (Zeng et al. 2000; Aravind et al. 2012) did not satisfy the orbital altitude constraints of the LEO departure and the retro-GEO insertion. The purpose of this paper is to discover the fundamental properties of the transfers in a three-body model, such as, whether the transfer with the free-return manner using the lunar swing-by is existed or not? What is the maximum altitude of the perilune of the transfer? How much is the orbital inclination changeable capacity of the transfer? After the concise statement of the problem in Sect. 2, the first two questions are exhibited in Sect. 3, and the last question is exhibited in Sect. 4. The paper ends with Sect. 5 which gives some brief conclusions and implications on this topic.

2 Problem statement

2.1 Advantages using lunar swing-by

If the retro-GEO satellite is deployed directly by the westward-launch manner for China, there are two problems. First, the most satellites of China launched up using an eastward-launch manner, there is no conventional landing area for the first and second stage-debris of the westward-launch rockets. The sub-points of the first and second stage-debris of the westward-launch rockets may spread to the densely populated area and even out of border. Second, the eastward-launch manner can be accurately measured and controlled by the mature ground stations of *China Xi'an Satellite Control Center*, while the westward-launch cannot be supported by mature stations. Moreover, the radius of the Earth is about 6378.134 km, and its rotation angular velocity is about 7.292115×10^{-5} rad/s. The beneficial velocity-increment of the eastward-launch manner launched-up from the equator is about 465 m/s, while there is about additional 465 m/s velocity-increment needs to be overcome using the westward-launch manner. It is a great difference fuel-cost of the about 930 m/s of the two manners.

The moon is the Earth's sole natural celestial body and is the most man-made probes visited

celestial body by-far. In particular, the Chang'e-series lunar probes of China shows that China has mastered the techniques of the lunar probes launch-up, precise orbit determination, and, orbital control around the Moon and return to the Earth surface.

2.2 Orbital dynamics and constraints

A simplified and classical orbital dynamics model to describe the path of a probe in the Earth-Moon space is the circular restricted three-body problem (CR3BP) model. In the CR3BP model, there are two primary bodies $[P_1, P_2]$ and the probe P of masses $m_1 > m_2 \gg m$, respectively. The motion of $[P_1, P_2]$ is not affected by the probe P, and move around their common center of mass under their mutual gravity. In the Earth-Moon space, $[P_1, P_2]$ represent the Earth and the Moon, respectively. Let $\mu = m_2/(m_1 + m_2)$ denotes the mass ratio of P_2 to the total mass. The motion of the probe P relative to a co-rotating coordinate system O-xyz as shown in Fig. 2 with the origin at their common center, and in normalized distance, mass, time units, and speed unit are described as shown in equation (1) and Tab. 1.

Tab. 1 Earth-moon space constants (He & Shen 2020)

Symbol	Value	Units	Meaning
μ	1.21506683×10^{-2}	-	Earth-moon mass ratio
l	1	m	Earth - moon distance unit
ω_z	1	s^{-1}	Earth - moon angular velocity unit
R_e	6378	km	Mean earth's radius
R_m	1738	km	Mean moon's radius
DU	3.84405000×10^{8}	m	Distance unit
TU	4.34811305	days	Time unit
VU	1.02323281×10^{3}	m s^{-1}	Speed unit

$$\ddot{x} - 2\dot{y} = \frac{\partial \Omega}{\partial x}, \ddot{y} + 2\dot{x} = \frac{\partial \Omega}{\partial y}, \ddot{z} = \frac{\partial \Omega}{\partial z} \tag{1}$$

Here the effective potential, Ω, is described as

$$\Omega = \frac{1}{2}\left(x^2 + y^2 + z^2\right) + \frac{1-\mu}{r_1} + \frac{\mu}{r_2} + \frac{1}{2}\mu(1+\mu) \tag{2}$$

with $r_1 = \sqrt{(x+\mu)^2 + y^2 + z^2}$, $r_2 = \sqrt{(x+\mu-1)^2 + y^2 + z^2}$ in (2). $[P_1, P_2]$ are located at $(-\mu, 0, 0)$, $(1-\mu, 0, 0)$, respectively.

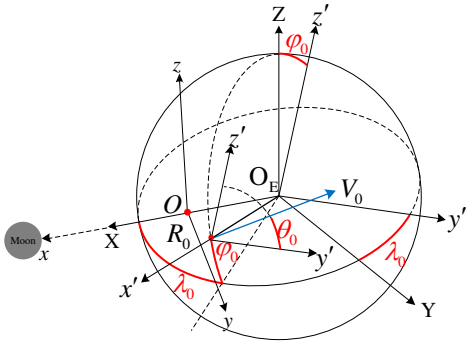

Fig. 2 Illustration of the vectors of the position and velocity of trans-lunar injection

Select the moment of the trans-lunar injection (i.e., the subscript '0' means the start epoch) as the epoch of the Earth-centered instantaneous inertial coordinate system O_E-XYZ, O_E-X points to the center of the Moon, O_E-Z points to the angular-momentum direction of the Moon's path, O_E-Y constructs the Cartesian coordinate system with the other two axes. In the coordinate system of O_E-XYZ, the vectors of the position and velocity $[\boldsymbol{R}_0, \boldsymbol{V}_0]$ are described as (3).

$$\begin{cases} \boldsymbol{R}_0 = R_0 \cdot \boldsymbol{M}_z(-\lambda_0)\boldsymbol{M}_y(\varphi_0)\cdot[1 \quad 0 \quad 0]^T \\ \boldsymbol{V}_0 = V_0 \cdot \boldsymbol{M}_z(-\lambda_0)\boldsymbol{M}_y(\varphi_0)\cdot[0 \quad \cos\theta_0 \quad \sin\theta_0]^T \end{cases} \tag{3}$$

Here, R_0 and V_0 describe the magnitudes of the vectors of the position and velocity respectively. λ_0 and φ_0 describe the directions of the vectors of the position respectively. θ_0 describes the direction of the vector of the velocity. $\boldsymbol{M}_y$ and $\boldsymbol{M}_z$ are the fundamental coordinate transformation matrixes, the other one $\boldsymbol{M}_x$ does not be used here. The obvious constraint is satisfied as $\mathrm{dot}(\boldsymbol{R}_0, \boldsymbol{V}_0) = 0$ means the velocity increment of the trans-lunar injection is tangential.

In the CR3BP model, O denotes the origin of the co-rotating coordinate system O-xyz. O-x follows the direction of the Moon's center. O-z follows the angular-momentum direction of the Moon's path. O-y constructs the active Cartesian coordinate system with the other two axes. The vectors of the position and velocity in O-xyz have constraints as (4).

$$\begin{cases} \boldsymbol{R}_0 = \boldsymbol{r}_0 + [\mu \quad 0 \quad 0]^T \\ \boldsymbol{V}_0 = \boldsymbol{v}_0 + \boldsymbol{\omega} \times \boldsymbol{r}_0 \end{cases} \tag{4}$$

Here $\boldsymbol{r}_0 = [x, y, z]_0^T$, $\boldsymbol{v}_0 = [\dot{x}, \dot{y}, \dot{z}]_0^T$, $\boldsymbol{\omega} = [\omega_x, \omega_y, \omega_z]^T = [0,0,1]^T$. And the additional rotation velocity is given by

$$\boldsymbol{\omega}\times\boldsymbol{r}_0=\begin{bmatrix}0 & -\omega_z & \omega_y\\ \omega_z & 0 & -\omega_x\\ -\omega_y & \omega_x & 0\end{bmatrix}\boldsymbol{r}_0 \tag{5}$$

Similarly, select the moment of the perigee of the final return phase (i.e., the subscript 'f' means the final epoch) as the final epoch of the transfer. The vectors of the position and the velocity at this moment satisfy the constraint of $\mathrm{dot}\left(\boldsymbol{R}_\mathrm{f},\boldsymbol{V}_\mathrm{f}\right)=0$.

Besides, another constraint is that the perilune altitude of the transfer is more than zero at least.

3 Properties in the planar three-body model

3.1 Existential analysis

Considering that the transfers solved by the previous work (Zeng et al. 2000; Aravind et al. 2012) did not completely satisfy the constraints, an explanation of the existence of this transfer without middle way maneuver is firstly given. The six-dimensional phase space of this transfer offers the perfect demonstration of the existential explanation, but Poincaré proves that there is no analytical mathematical procedure to the transfers in the three-body problem. And then, he suggested the Poincaré-section map methodology, it can give a clear criterion and qualitative conclusions for the problems in the three-body problem. Refer to the author's previous work experience (He & Shen 2020) , the planar three-body model is used flexibly to obtain its fundamental features. In other words, the planar three-body model is a dimension-reduced result of (1), the O-z direction is decoupled from the other two directions in O-xyz. To be specific, the orbital element $[\varphi,\theta]$ are neglected in the full time.

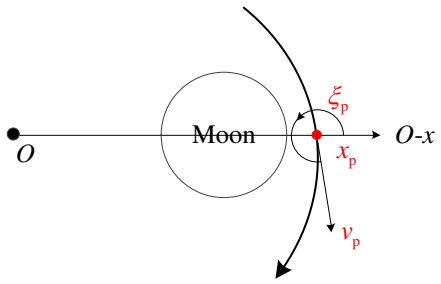

Fig. 3 Illustration of the Poincaré-section map

Select the orbital elements at the moment of trans-lunar injection and the moment of the perigee of the final return phase as the traversal searching variables, respectively. The trans-lunar phase is calculated using the numerical integration in the positive direction of time, while the trans-earth phase

is calculated using the numerical integration in the negative direction of time. Both stop at the Poincaré-section. The Poincaré-section is selected here at the axis of O-x and is far-away from the Earth and the Moon. It has three orbital elements as shown in Fig. 3, the value of the position on O-x of x_{p}, the value of the velocity magnitude of v_{p}, and, the value of the velocity angle of ξ_{p}, all of them is at the moment when the value of the position component of O-y is zero (i.e., $y_{\mathrm{p}}=0$). The subscript 'p' denotes the perilune vicinity.

The geocentric distance R_0 at the moment of trans-lunar injection is used to being a constant, because it is dominated by the capability of the rocket. The geocentric distance R_{f} at the moment of the perigee of the final return phase is the same with that of the GEO. The existential analysis of this transfer is explained using the selected Poincaré-section map to an appointment problem as shown in Fig. 4. The orbital elements $\left[x_{\mathrm{p}},v_{\mathrm{p}},\xi_{\mathrm{p}}\right]^{+}$ computed from $\left[R_0,\lambda_0,V_0\right]$ by the numerical integration in the positive directions of time, and $\left[x_{\mathrm{p}},v_{\mathrm{p}},\xi_{\mathrm{p}}\right]^{-}$ computed from $\left[R_{\mathrm{f}},\lambda_{\mathrm{f}},V_{\mathrm{f}}\right]$ by the numerical integration in the negative directions of time, respectively, meet on the Poincaré-section map at the moment of $y_{\mathrm{p}}=0$. If there is a non-empty intersection set about $\left[x_{\mathrm{p}},v_{\mathrm{p}},\xi_{\mathrm{p}}\right]^{+}$ and $\left[x_{\mathrm{p}},v_{\mathrm{p}},\xi_{\mathrm{p}}\right]^{-}$, the existence of this transfers is sufficiently proven. Otherwise, there is no transfer without middle way maneuver in the planar three-body model.

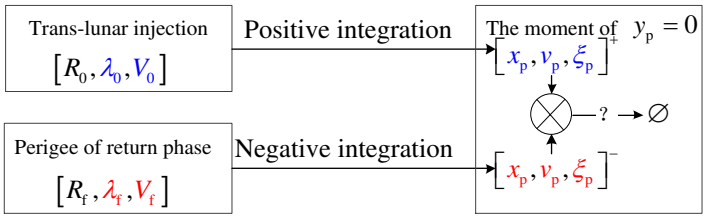

Fig. 4 Illustration of the existential analysis strategy

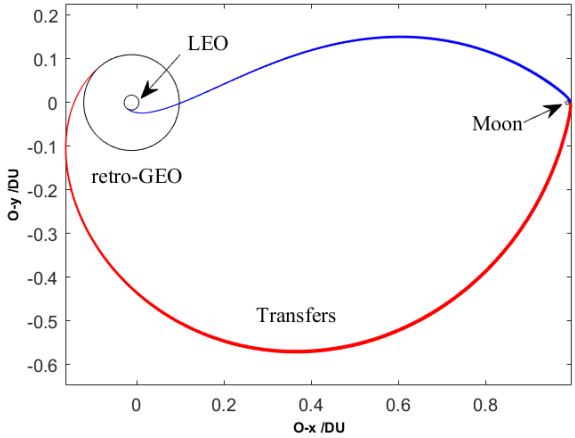

Fig. 5 The planar trajectories of the transfers

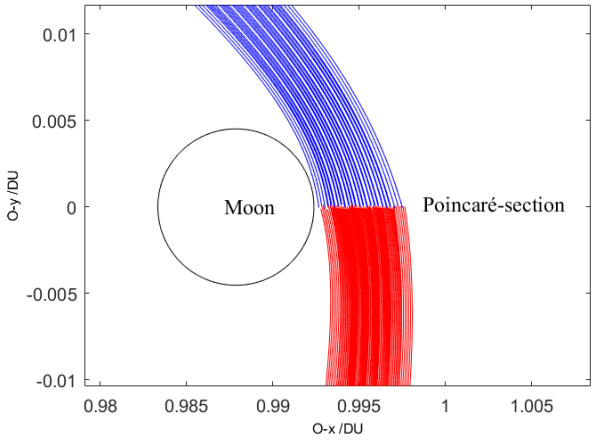

Fig. 6 The partial enlarged detail trajectories of the Poincaré-section

Tab. 2 Earth-moon space constants

Computing orbit elements		Results of Poincaré-section map	
Symbol	Value/Units	Symbol	Value/Units
R_0	6545 /km	x_p^+	[0.9926,0.9975] /DU
λ_0	[225.1,225.4] /deg	v_p^+	[0.3377,0.5615] /VU
V_0	[10.9838,10.985] /km·s^{-1}	ξ_p^+	[-82.4637,-73.9266] /deg
R_f	42164 /km	x_p^-	[0.9928, 0.9976] /DU
λ_f	[126.5,127.3]/deg	v_p^-	[0.3190,0.6998] /VU
V_f	[4.1261,4.1271] /km·s^{-1}	ξ_p^-	[-81.4566,-74.6909] /deg

Without loss of generality, set $R_0 = 6545$ km (i.e., 6378+167) (He & Shen 2020), and set R_f =

42164 km (i.e. 6378+35786). The orbit elements on the Poincaré-section map and the computing orbit elements are listed in Tab. 2. The planar trajectories of the transfers are shown in Fig. 5, and its partial detail trajectories enlarged of the Poincaré-section are shown in Fig. 6. The three-dimensional parameter Poincaré-section map and its three plane views of the inter-section listed in Tab. 2 are plotted in Fig. 7 (a,b,c,d), the blue box denotes $\left[x_{\mathrm{p}}, v_{\mathrm{p}}, \xi_{\mathrm{p}}\right]^{+}$ of the trans-lunar phase while the red five-pointed star denotes $\left[x_{\mathrm{p}}, v_{\mathrm{p}}, \xi_{\mathrm{p}}\right]^{-}$ of the trans-earth phase.

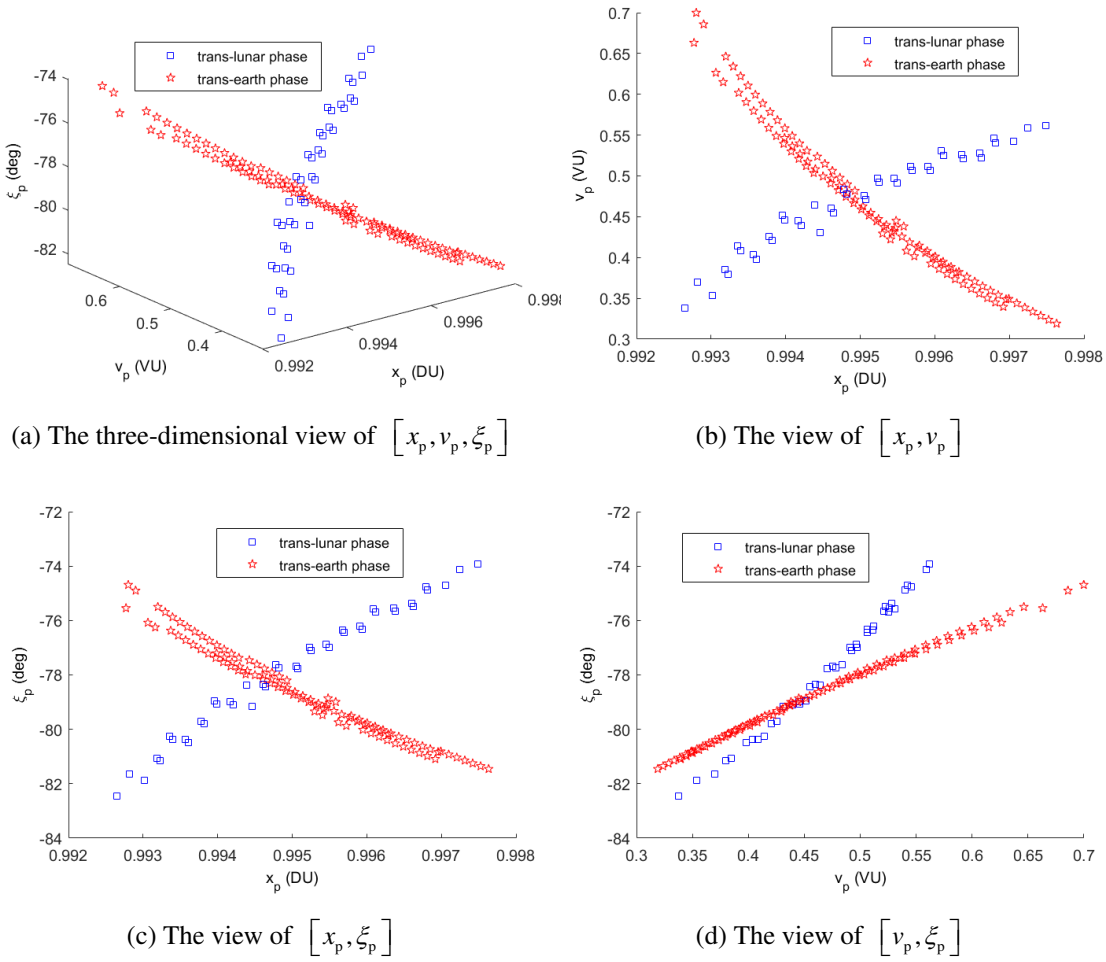

(a) The three-dimensional view of $\left[x_{\mathrm{p}}, v_{\mathrm{p}}, \xi_{\mathrm{p}}\right]$

(b) The view of $\left[x_{\mathrm{p}}, v_{\mathrm{p}}\right]$

(c) The view of $\left[x_{\mathrm{p}}, \xi_{\mathrm{p}}\right]$

(d) The view of $\left[v_{\mathrm{p}}, \xi_{\mathrm{p}}\right]$

Fig.7 The three-dimensional parameter Poincaré-section map

It is clearly obtained the existential explanation from the non-empty set demonstration that the transfer from LEO to the retrograde-GEO using lunar swing-by without middle way maneuvers in the three-body model exists.

3.2 Limit of the perilune altitude

In the Poincaré-section map of the primary computing results in Sect. 3.1, it appears a phenomenon that the perilune altitude of the transfers within the two strict perigee altitude constraints

is limited to an upper-bound. For solving this limit value of the upper-bound, a simple optimization model is suggested as (6). This optimization problem is essentially looking for the transfer with the maximum value of the perilune altitude in the solution set as shown in Sect. 3.1. And the SQP (sequence quadratic programming) algorithm in the Matlab *fmincon* function is applied here, since the initial value of the design variables is obtained in Sect. 3.1. The iteration process is convergent to 1×10^{-4} with a number of iteration which is less than 20, the limit value of the perilune altitude is about 892.2 km as shown in Fig. 8. The values of this transfer's design variables are listed in Tab. 3.

$$\begin{cases} \boldsymbol{x}=\left[\lambda_0, V_0, \lambda_{\mathrm{f}}, V_{\mathrm{f}}\right] \\ \text{s.t.}\begin{cases} y_{\mathrm{p}}^{+}=y_{\mathrm{p}}^{-}=0 \\ x_{\mathrm{p}}^{+}=x_{\mathrm{p}}^{-} \\ v_{\mathrm{p}}^{+}=v_{\mathrm{p}}^{-} \\ \xi_{\mathrm{p}}^{+}=\xi_{\mathrm{p}}^{-} \end{cases} \\ \min J=-x_{\mathrm{p}}^{+} \end{cases} \tag{6}$$

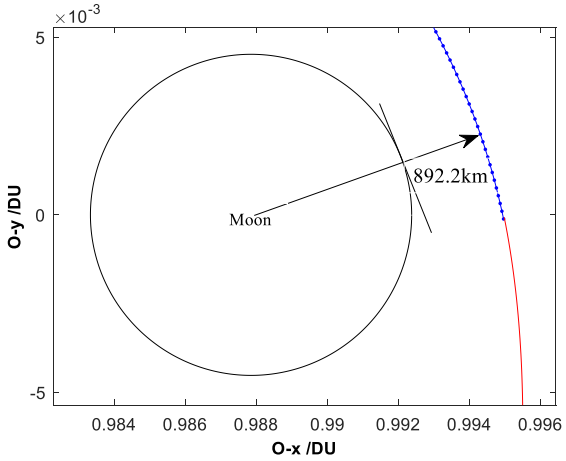

Fig. 8 Limit of the perilune altitude

Tab. 3 The values of the transfer's design variables with the highest perilune altitude

Variables/Units	λ_0 /deg	V_0 /km·s^{-1}	λ_{f} /deg	V_{f} /km·s^{-1}
Values	225.280236	10.983999	126.796756	4.126486

4 Properties in the spatial three-body model

4.1 The continuation method from planar to spatial

In reality, the direct purpose of this transfer using lunar swing-by is to change the orbital inclination from a direct orbit to a retro-GEO orbit in the Earth-centric view. The orbital inclination-changeable capacity of this transfer in the spatial three-body model is suggested to be solved using the continuation method from the results in the planar three-body model. In the planar

three-body model, the most transfers have duration of 1.64654 TU (i.e., the sum of the 0.584 TU for trans-lunar phase and the 1.062 TU for trans-earth phase). Here the duration and the values of the transfer's design variables in Tab. 3 are applied to play the sectional initial values of the orbital design variables. The solving model in the spatial three-body model is suggested as follow.

$$\begin{cases} search \quad \left(\left[\theta_{\mathrm{f}} = \theta_{\mathrm{f}}^{\min} \right] \leftarrow \left[\theta_{\mathrm{f}} = \pi \right] \rightarrow \left[\theta_{\mathrm{f}} = \theta_{\mathrm{f}}^{\max} \right] \right) \\ \begin{cases} \boldsymbol{x} = \left[\lambda_0, \varphi_0, V_0, \theta_0, \Delta t, \lambda_{\mathrm{f}}, \varphi_{\mathrm{f}}, V_{\mathrm{f}} \right] \\ \min J = \left(\left| \vec{\boldsymbol{r}}_{\mathrm{mid}} - \vec{\boldsymbol{r}}_{\mathrm{mid}} \right| + \left| \vec{\boldsymbol{v}}_{\mathrm{mid}} - \vec{\boldsymbol{v}}_{\mathrm{mid}} \right| \right) < \varepsilon \end{cases} \\ end \end{cases} \tag{7}$$

In this extended dimensional solving model, the direction angle of the vector of the velocity θ_{f} at the moment of the retro-GEO insertion is selected to be the continuation parameter, because it is the most prominent parameter affecting the inclination changeable capacity. Its value is π in the planar three-body model in default, hence its value changes to its minimum and maximum boundaries from π with a small step $\Delta\theta_{\mathrm{f}}$ using the numerical continuation methodology as the utilization in our previous work (He & Shen 2020). The initial values of the extended variable $\left[\varphi_0, \theta_0, \varphi_{\mathrm{f}}\right]$ are zeros, and the initial value of Δt is a half of 1.64654 TU. The arrows on the head of $(\boldsymbol{r}, \boldsymbol{v})$ mean the end states of the integral procedure using direct and retrograde time sequences, and the subscript 'mid' means these two integral procedures both stop at the middle of the whole fight duration. The slice of the integral procedure is used to being a technique for reducing the sensitivity of a non-linear dynamics system, and it is sometimes called shooting method (Topputo 2013). ε is the convergence threshold of the optimization process.

4.2 The orbital inclination changeable capacity

With an optioned value $\Delta\theta_{\mathrm{f}}$ = 1 degree and ε = 1×10^{-3}, the optimal results of the orbital design variables are used to be the initial values of the next new optimization in equation (7). After the two serial optimization processes of $\left[\theta_{\mathrm{f}} = \pi\right] \rightarrow \left[\theta_{\mathrm{f}} = \theta_{\mathrm{f}}^{\min}\right]$ and $\left[\theta_{\mathrm{f}} = \pi\right] \rightarrow \left[\theta_{\mathrm{f}} = \theta_{\mathrm{f}}^{\max}\right]$ continual and parallel ended up, all the transfers are obtained by the utilization of the SQP algorithm mentioned in section 3.2. Their trajectories are shown in Fig. 9.

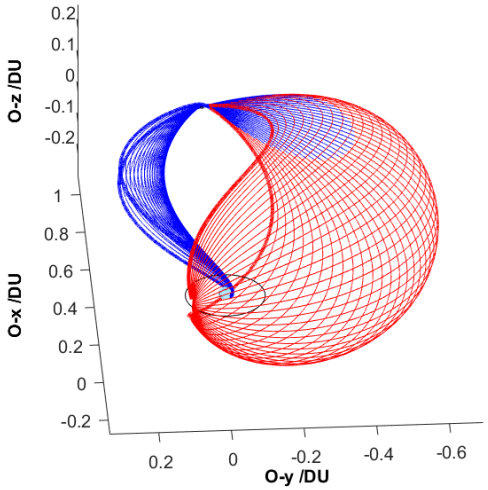

Fig. 9 Trajectories of the spatial transfers

The values of $\theta_{\mathrm{f}}^{\min}$ and $\theta_{\mathrm{f}}^{\max}$ are 42 degree and 318 degree respectively, the trajectories of this two transfers are special plotted in a bold line style. All the solution is strictly symmetric of the plane of x-O-y, it displays the symmetrical features of the existence of the transfers in the spatial CR3BP model proven by (Miele & Mancuso 2001). The positions at the moment of retro-GEO insertion have a small and symmetric dispersion as plotted in Fig. 10. This feature illustrates the selection of the continuation parameter θ_{f} is proper and imperative. The minimum and maximum values of θ_{f} both deviates from its initial value $\theta_{\mathrm{f}}=\pi$ with an orbital inclination changeable capacity of 138 degree. This natural property has a significant application to explain the trans-lunar month windows, due to the maximum angle of the plane of the Moon's path on the equator is 28.6 degree per Metonic cycle (i.e., 18.6 years), so everyday has a month window to match the longitude of the launch-site for trans-lunar injection.

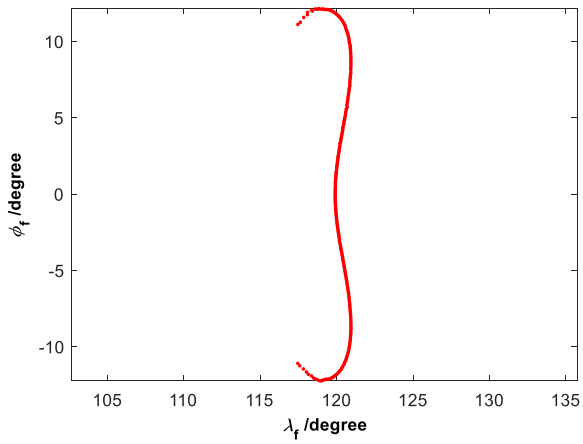

Fig. 10 Distribution of the positions at the moment of retro-GEO insertion

4.3 The minimum sum of the two-impulse velocity increments

For a general space mission, the impulsive sum of the velocity increments from a LEO departure is considered to be an important evaluation index. The value of this transfer consists of two parts, one is the velocity increments of departure from a LEO, and another is the velocity increments of inserting into a retro-GEO as (8).

$$\Delta V_{\text{total}} = \left(V_0 - \sqrt{\mu_{\text{E}}/R_0}\right) + \left(V_{\text{f}} - \sqrt{\mu_{\text{E}}/R_{\text{f}}}\right) \tag{8}$$

Here, $\mu_{\text{E}} = 3.9860044 \times 10^5 \,\text{km}\cdot\text{s}^{-1}$ is the Earth's gravitational constant in an inertial coordinate system. It is relative to θ_{f} as shown in Fig. 11. The minimum value of the sum of the two-impulse velocity increments (i.e., depart from LEO and insert into the retro-GEO) is 4.224 km/s, and occur in the two cases, θ_{f} = 73 degree and θ_{f} = 287 degree. In other words, the change of the orbital inclination is 107 degree relative to the plane of the Moon's path in these two cases.

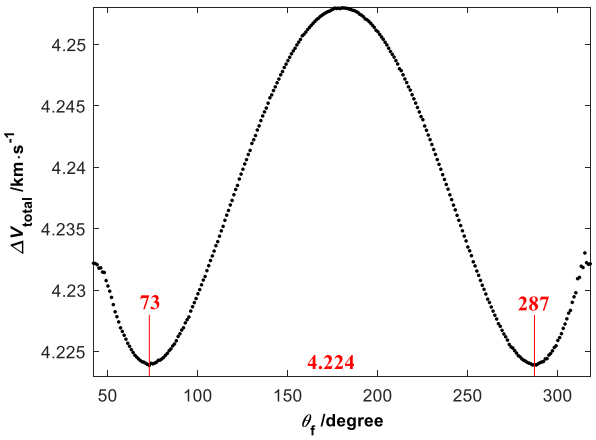

Fig. 11 The sum of the two-impulse velocity increments

5 Conclusions

The properties of the transfers from LEO to the retrograde-GEO using lunar swing-by in CR3BP model are calculated and exhibited in this work. The conclusions are drawn as follows:

(1) The transfer constrained with the altitudes of departing from LEO and of inserting into retro-GEO is existential using lunar swing-by without middle-way impulse.

(2) The maximum limit of the perilune altitude is 892 km.

(3) The orbital inclination changeable capacity is 138 degree relative to the plane of the Moon's path. Everyday has a month window to match the longitude of the launch-site for trans-lunar injection.

(4) The minimum value of the sum of the two-impulse velocity increments of this transfer is 4.224

km/s, and these two cases occur in the change of the orbital inclination is 107 degree relative to the plane of the Moon's path.

Extensive numerical calculations have been done in this work. The obtained results reveal some natural properties of this transfer and provide references to design a transfer using perturbed orbital dynamics model of deploying a monitor-satellite on the retro-GEO for debris-warning mission.

Acknowledgements

This work was supported by the National Natural Science Foundation of China (No. 11902362) and the China Postdoctoral Science Foundation (No. 2020M683764).

Reference

Aravind, R., Harsh, S., Bandyopadhyay, P.: Mission to retrograde geo-equatorial orbit (RGEO) using lunar swing-by. IEEE Aerospace Conference. (2012)

Berry, R. L.: Launch window and trans-lunar orbit, lunar orbit, and trans-earth orbit planning and control for the Apollo 11 lunar landing mission. AIAA 8th Aerospace Sciences Meeting, New York. No.70-0024 (1970)

Espinosa, S. A.: Two new satellites now operational expand U.S. space situational awareness. Air Force Space Command Public Affairs (2017-09-13) http://www.afspc.af.mil. Cited 8 Sep 2020

Farquhar, R. W.: The flight of ISEE-3/ICE: origins, mission history, and a legacy. J. Astronaut. Sci. **49**(1), 23–73 (2001).

He, B. Y., Shen, H. X.: Solution set calculation of the sun-perturbed optimal two-impulse trans-lunar orbits using continuation theory. Astrodynamics. **4**(1), 75–86 (2020)

Kawase, S.: Retrograde satellite for monitoring geosynchronous debris. 16th International Symposium on Space Flight Dynamics, Pasadena, California, USA. pp. 3-7 (2001)

Kawase, S.: Retrograde satellite to monitor overcrowded geosynchronous orbits. J-JSASS. **673**(58), 31-37 (2010).

Luo, Z. F., Meng, Y. H., Tang, G. J.: Solution space analysis of double lunar-swingby periodic trajectory. Sci. China Technol. Sci. **53**(8), 2081-2088 (2010)

Miele, A., Mancuso, S.: Optimal trajectories for earth–moon–earth flight. Acta Astronaut. **49**(2), 59–71 (2001)

Oberg, J.: Pearl harbor in space. Omni Mag. **6**, 42-44 (1984)

Oltrogge, L. D., Alfano, S., Law, C. et al.: A comprehensive assessment of collision likelihood in

geosynchronous earth orbit. Acta Astronaut. **147**(6), 316–345 (2018)

Topputo, F.: On optimal two-impulse earth–moon transfers in a four-body model. Celest. Mech. Dyn. Astron. **117**(3): 279–313 (2013)

Uesugi, K.: Japanese fist double lunar swing-by mission "HITEN". 41st Congress of the International Astronautical Federation, No. 1990-343 (1990)

Zeng, G. Q., Xi, X. N., Ren, X.: A study on lunar swing-by technique. J. Astronaut. **21**(4), 107-110 (2000)

Figures

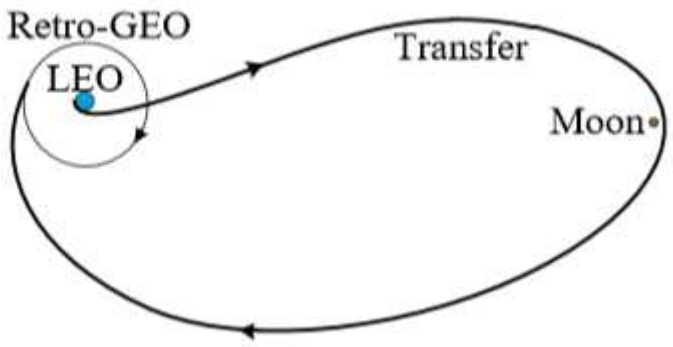

Figure 1

Illustration of the transfer from LEO to the retrograde-GEO using lunar swing-by

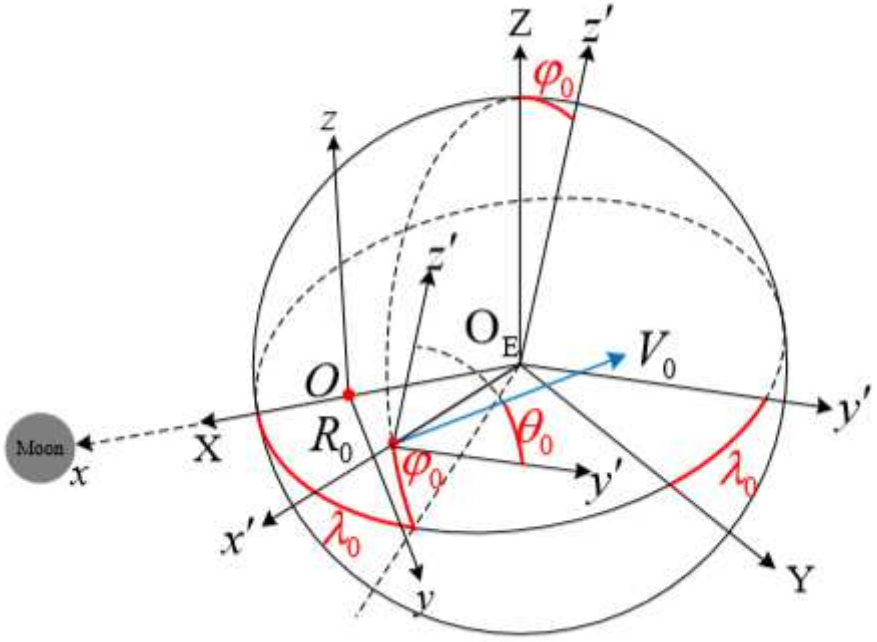

Figure 2

Illustration of the vectors of the position and velocity of trans-lunar injection

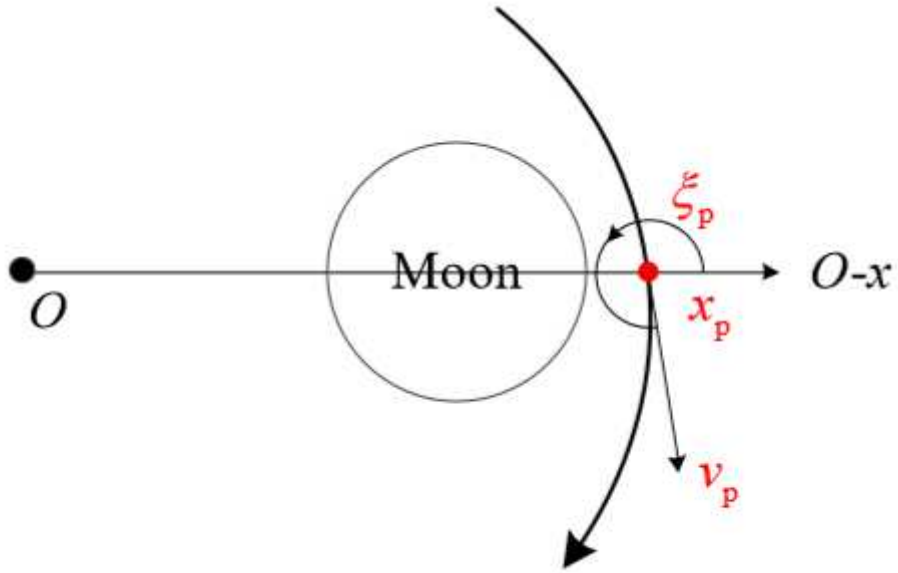

Figure 3

Illustration of the Poincaré -section map

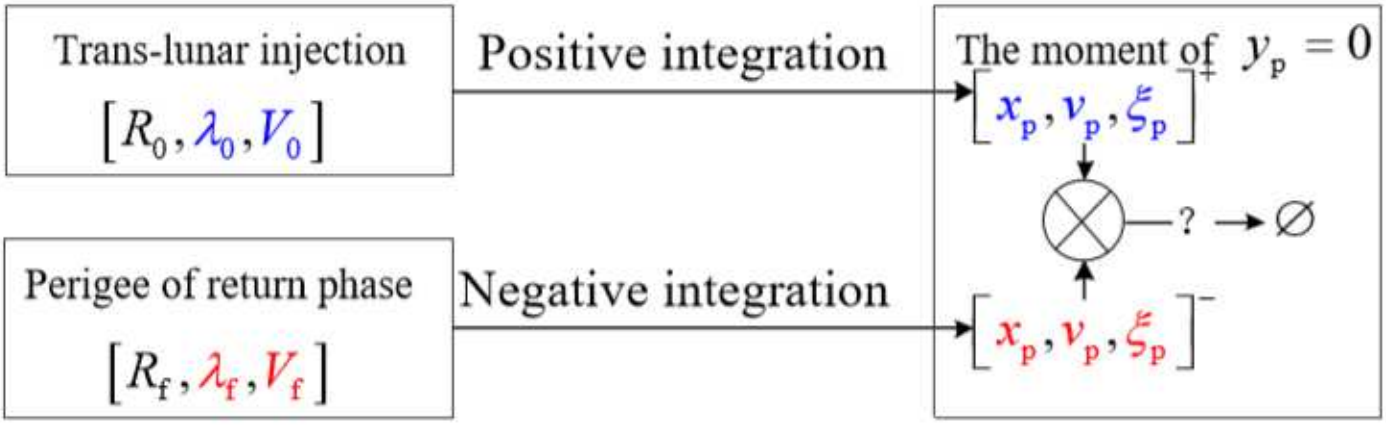

Figure 4

Illustration of the existential analysis strategy

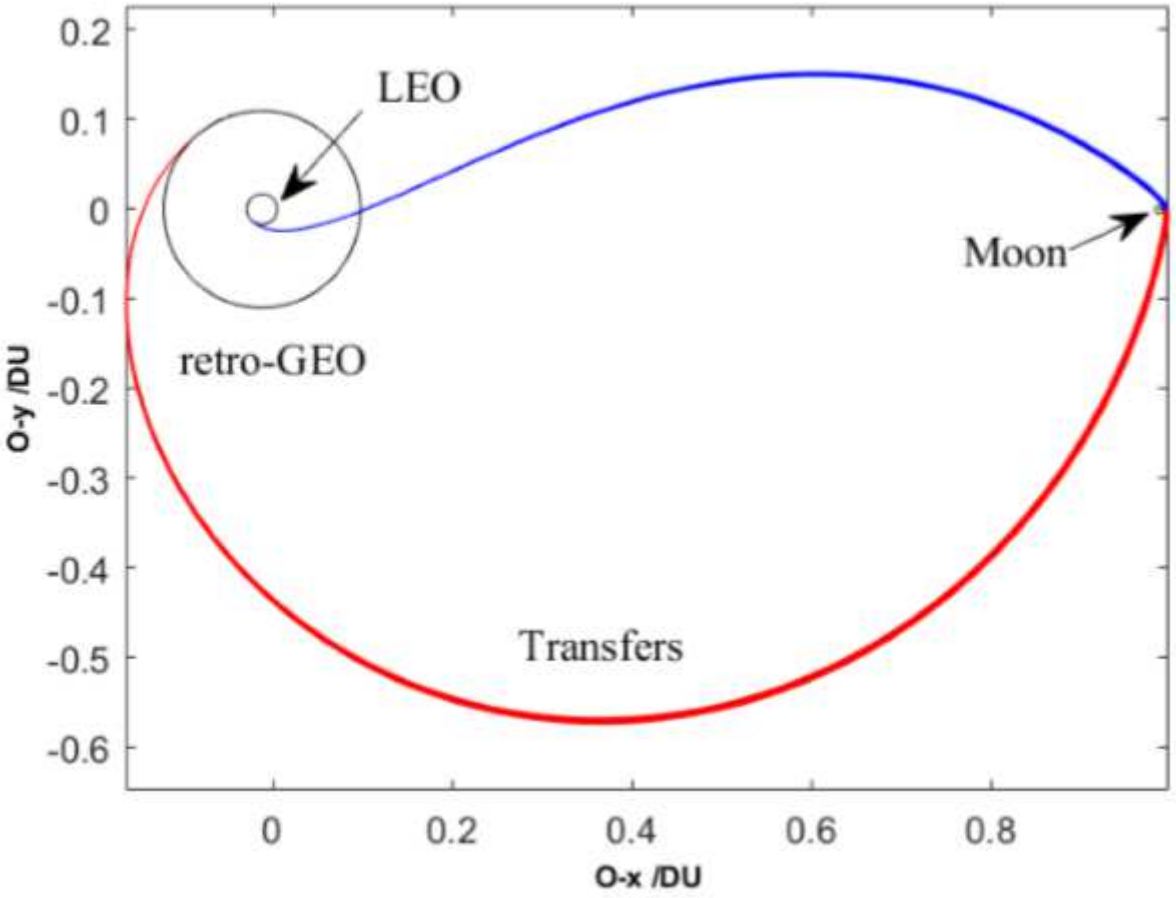

Figure 5

The planar trajectories of the transfers

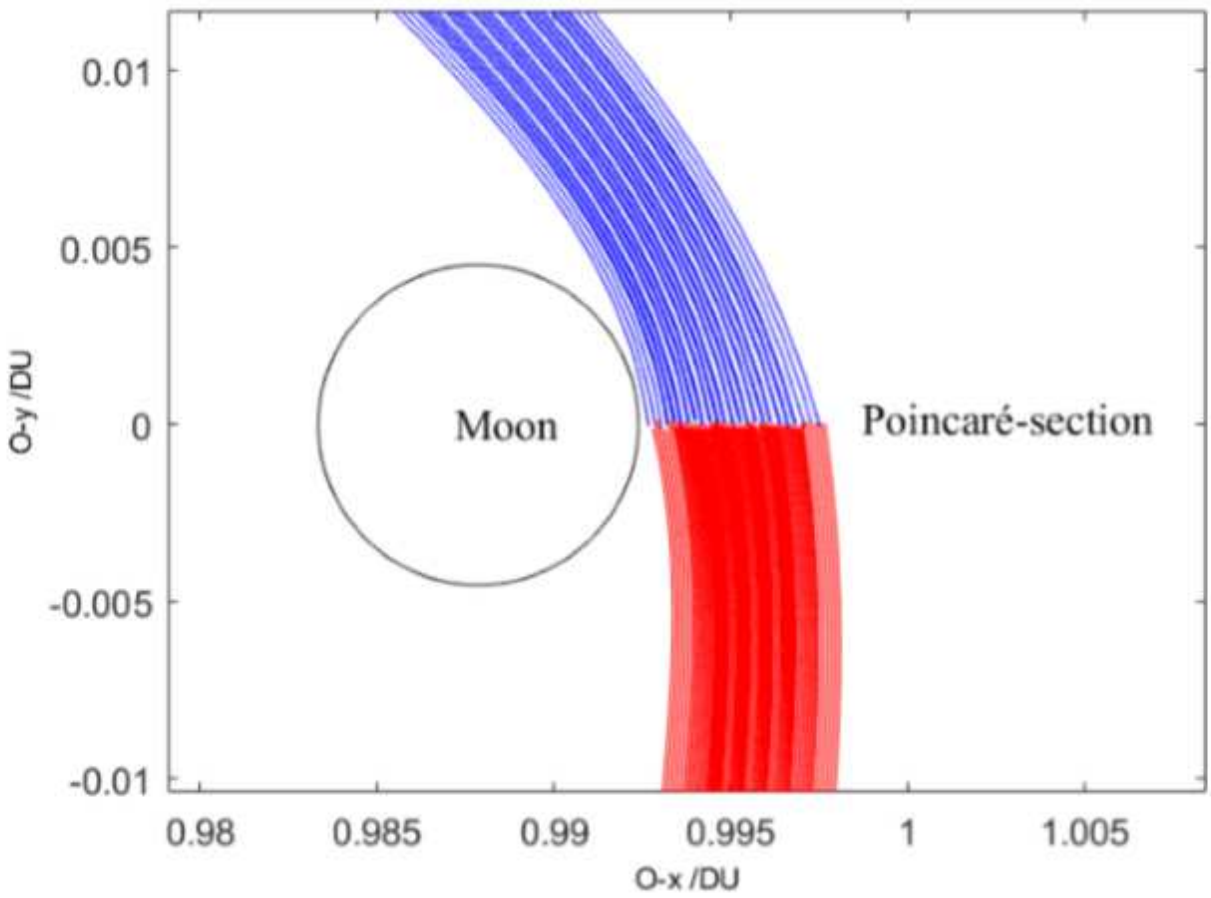

Figure 6

The partial enlarged detail trajectories of the Poincaré -section

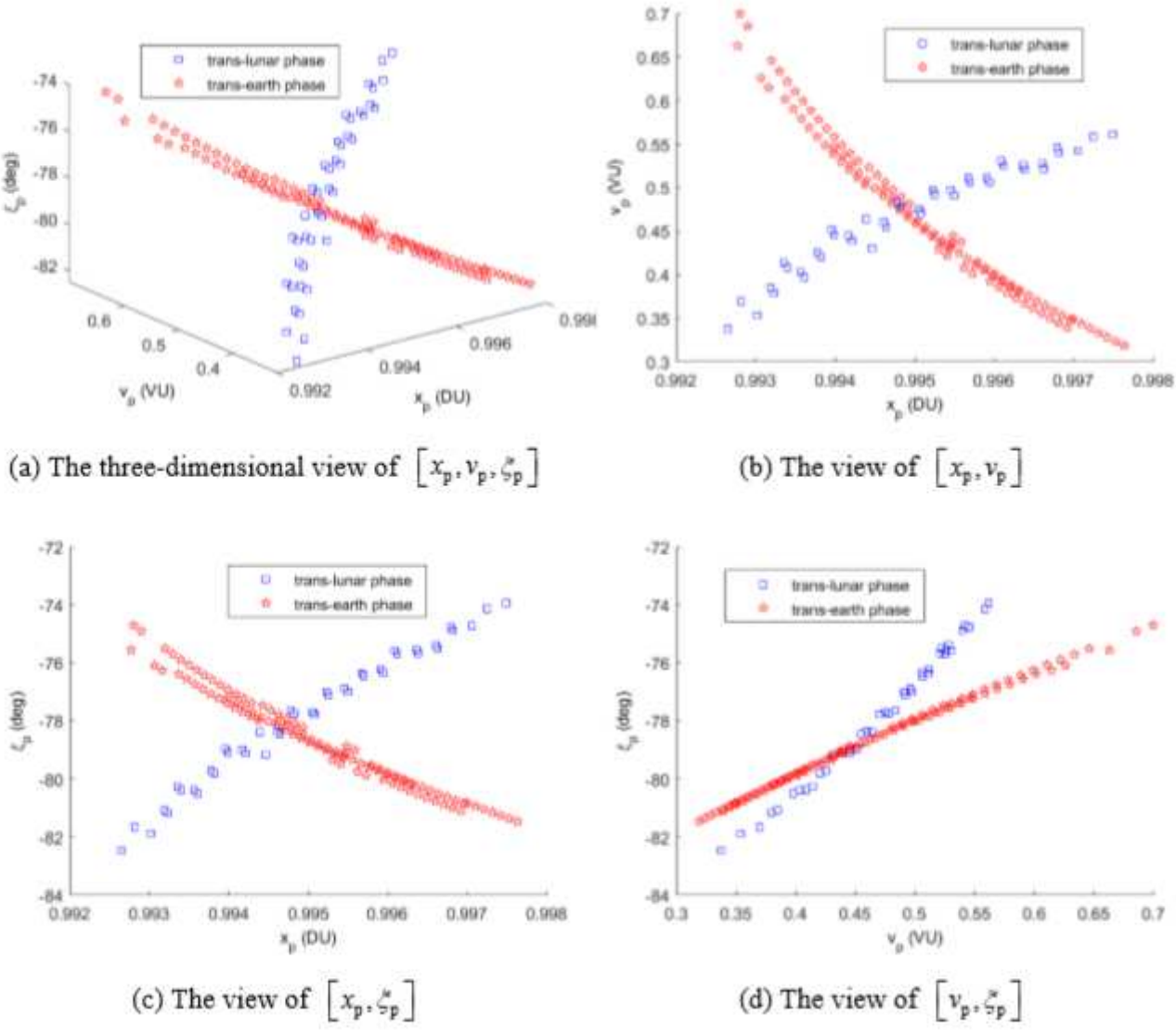

Figure 7

The three-dimensional parameter Poincaré -section map

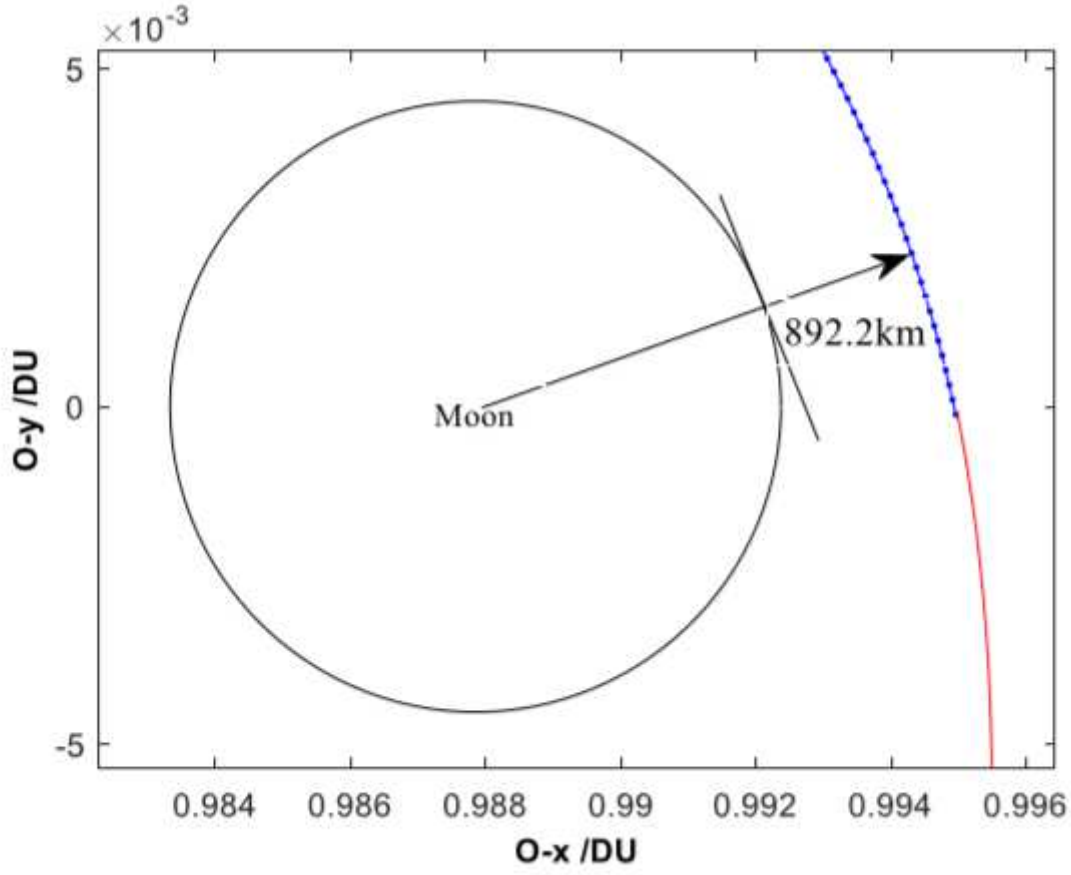

Figure 8

Limit of the perilune altitude

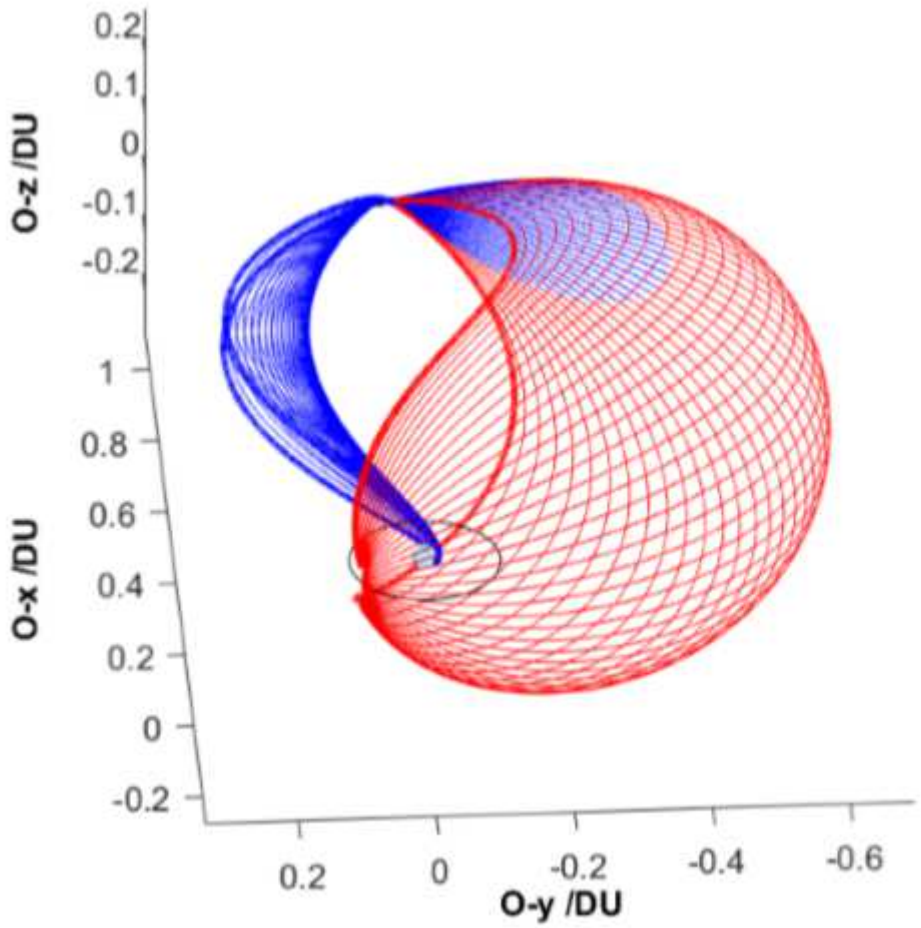

Figure 9

Trajectories of the spatial transfers

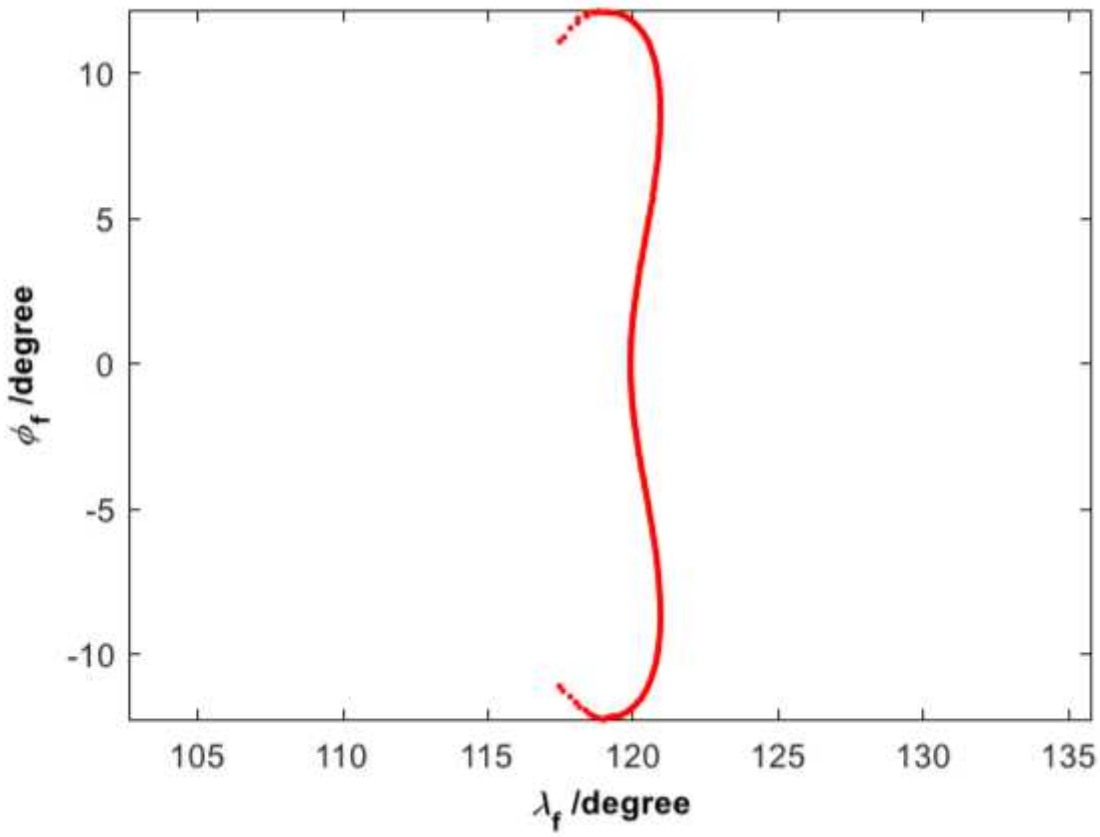

Figure 10

Distribution of the positions at the moment of retro-GEO insertion

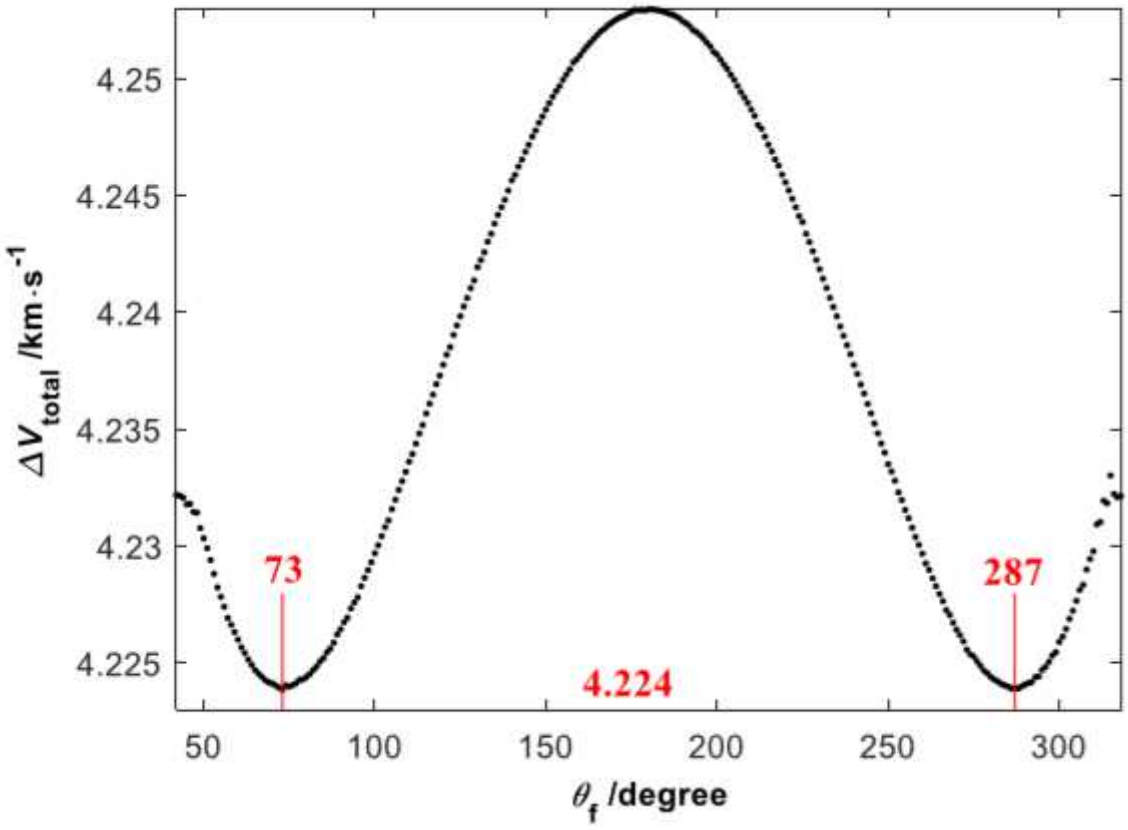

Figure 11

The sum of the two-impulse velocity increments

Supplementary Files

This is a list of supplementary files associated with this preprint. Click to download.

- tables.docx